Improved Knowledge of SAR Geomerty through Atmospheric Modelling

Michael Jehle, Othmar Frey, David Small, Erich Meier, Daniel Nüesch

Remote Sensing Laboratories (RSL) - University of Zürich
Winterthurerstrasse 190; CH-8057 Zürich; Switzerland
Tel: +41 +44 635-6516 / FAX: +41 +44 635-6842 / E-Mail: michael.jehle@geo.unizh.ch

Abstract

Satellites observing and measuring the Earth's surface with electromagnetic waves are subject to atmospheric path delays. Atmospheric effects on radar signal propagation modify the signal velocity and direction and can be considered by simple modelling. In order to increase the geolocation accuracy of spaceborne SAR applications we developed a software tool that accounts for atmospheric path delays. Well-calibrated spaceborne ENVISAT-ASAR data are used to investigate improvements to knowledge of the geometry of the scene

I. Introduction

Knowledge of range and azimuth in spaceborne SAR has improved in recent years. Regarding geometric accuracy, the importance of atmospheric path delay increases as well with continuing improvements to the resolution of SAR systems surveying the Earth and other planets. Contributions of path delay of the atmosphere must be respected in order to be able to get an atmosphere-independent geolocation accuracy in the range of approximately one meter. This motivated a study dedicated to geometric error budget analysis for the upcoming TerraSAR-X satellite [1].
Atmospheric path delay contributions are mainly due to ionospheric and tropospheric influences. **Figure 1** illustrates a simplified electromagnetic wave propagation through the atmosphere. At X-band frequencies, ionospheric path delay can amount [1] to up to 1 m and tropospheric delay up to 3 m only for propagation from the satellite to the Earth. For SAR systems this delay can add up to 16 m, when one compares two way path delays between ascending / descending acquisition geometries.

II. Ionospheric Delay

- Free electrons in the ionosphere affect the refractive index of the layer.
- The more free, electrons the higher the refractive index, the lower the signal velocity and the higher the resulting path delay through the ionosphere.
- **TEC** (Total Electron Content) is specified by number of free electrons in a column of 1 m^2 along signal path.
- Daily maps of global TEC are published on the internet (e.g. www.aiub.unibe.ch/ionosphere/)
- Path delay $\Delta\Psi_{iono,\ SAR}$ through ionosphere for electromagnetic waves travelling from a satellite to the Earth and back can be calculated by [2]:

$$\Delta\Psi_{iono,\ SAR} = 2 \cdot K \cdot \frac{TEC}{f^2 \cdot \cos\alpha_{OffNd}}$$

- Factor $\frac{1}{\cos\alpha_{OffNd}}$ accounts for slant range direction. α_{OffNd} [degrees] denotes the satellite off-nadir angle, and K=40.28$\left[\frac{m^3}{s^2}\right]$ is a refractive constant [2].
- Path delays for X-band frequencies can be in the range of up to 2 m for propagation through the ionosphere to the Earth and back.
- Ascending (ASC) / (DSC) intercomparisons double effect of the error.

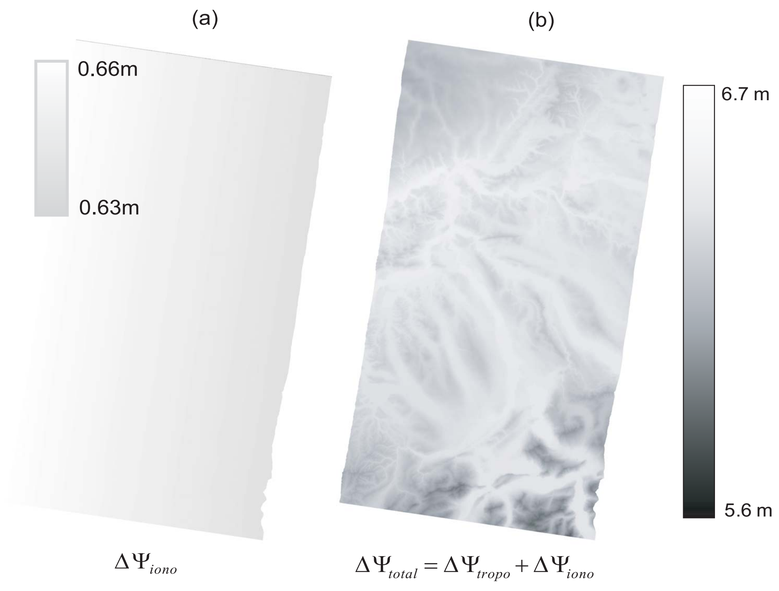

***Figure 2**: Ionospheric- (left) vs. total path delay (right).*

Predicting TEC is difficult due to the high variability of the ionosphere. An approach for a global TEC prediction model, looking a few days into future was developed by [3] and is implemented as an optional feature in the software tool for SAR-based atmospheric corrections. The basic idea is to extend the Klobuchar model [4] that estimates TEC using a daily cosine function, with periodic parameters that influence the daily TEC. According to measurements, it is mainly the periodicity due to the 11 year solar cycle, the lunar cycle and annual- and semi annual variations. Extrapolating and estimating a trend function of the parameters leads to a stand-alone TEC prediction model. The accuracy for long time period predictions is low due to the ionosphere's variability.
Figure 2 shows on the left (Figure 2a) an example of atmospheric path delay for a C-band ENVISAT-ASAR scene acquired on January 22th 2003 at 9:29 UTC. Modelled TEC was 18 TECU in zenithal direction and off-nadir angle was from 36.7 to 39.3 degrees. Calculated path delays range from 0.63 m to 0.66 m increasing with growing off-nadir angle. Figure 2b shows the calculated total atmospheric path delay. It can clearly be seen, that total path delay depends strongly on topography. The total path delay for C-band is typically in the range of 5 m to 7 m.

III. Tropospheric Delay

- Caused by variations in the refractive index *n* as a function of air pressure *P*, temperature *T*, and water vapour pressure *e*.
- Tropospheric delay is usually separated into a hydrostatic $\Delta\Psi_{\text{hydro, SAR}}$, a wet $\Delta\Psi_{\text{wet, SAR}}$, and a liquid $\Delta\Psi_{\text{liq, SAR}}$ component:

$$\Delta\Psi_{tropo,\ SAR} = \Delta\Psi_{hydro,\ SAR} + \Delta\Psi_{wet,\ SAR} + \Delta\Psi_{liq,\ SAR}$$

- $\Delta\Psi_{\text{hydro, SAR}}$ refers to a standard atmosphere, $\Delta\Psi_{\text{wet, SAR}}$ and $\Delta\Psi_{\text{liq, SAR}}$ model the difference between the standard and the actual atmosphere.
- $\Delta\Psi_{\text{wet, SAR}}$ accounts for water vapour, $\Delta\Psi_{\text{liq, SAR}}$ considers liquid water content (clouds, droplets) along signal path. Due to its small contribution (at cm level) $\Delta\Psi_{\text{liq, SAR}}$ is usually neglected.

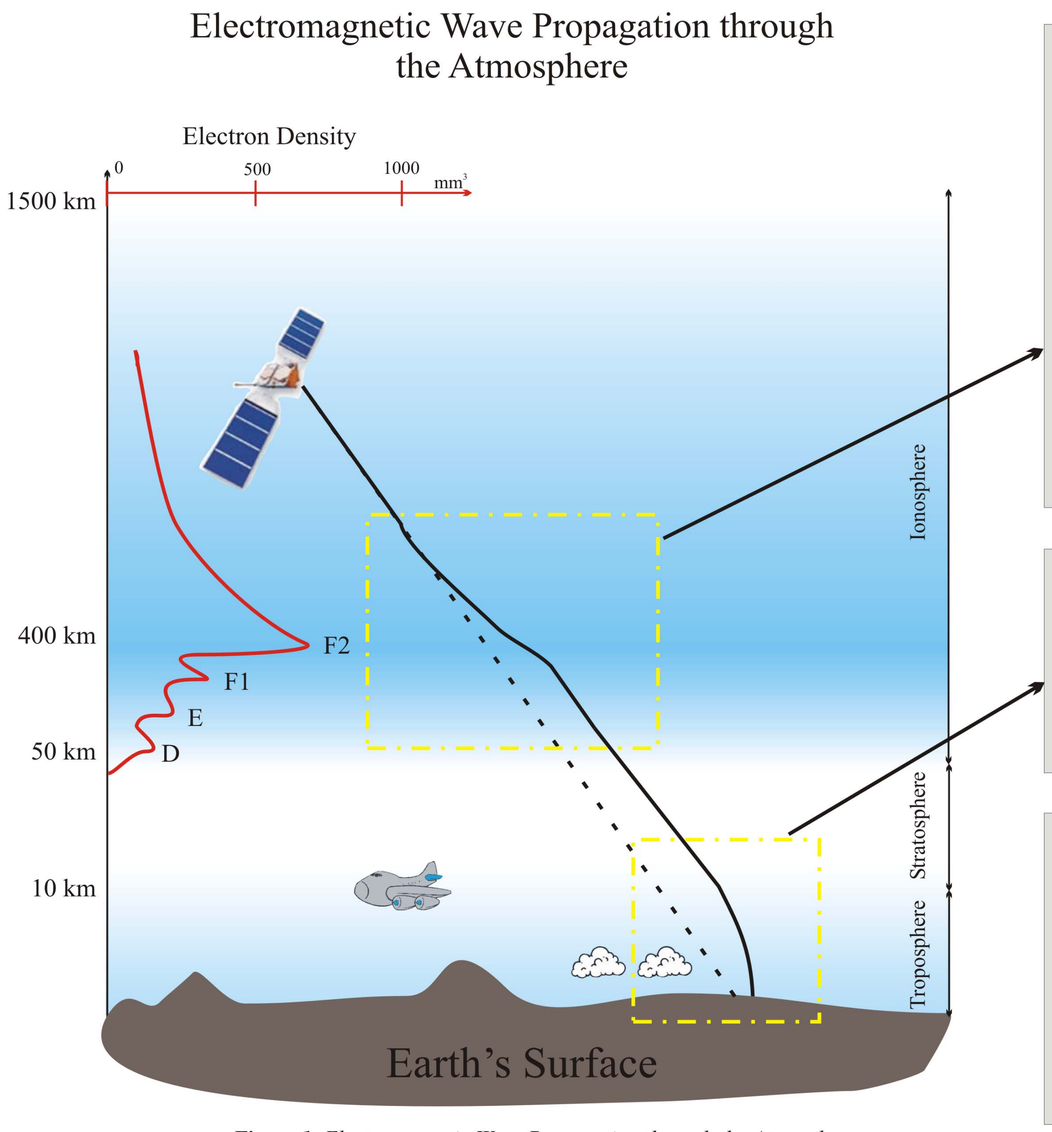

***Figure 1:** Electromagnetic Wave Propagation through the Atmosphere*

- As a function of the transformed refractive index $N = (n-1) \cdot 10^{-6}$ tropospheric path delay can be written as [2]:

$$\Delta\Psi_{tropo,\ SAR} = 2 \cdot \int_{path} N_{hydro} + N_{wet} + N_{liq}\, ds$$
$$= 2 \cdot 10^{-6} \int_{path} k_1 \frac{P}{T} ds + 2 \cdot 10^{-6} \int_{path} \left(k'_2 \cdot \frac{e}{T} + k_3 \cdot \frac{e}{T}\right) ds + 2 \cdot \Delta\Psi_{liq}$$

- The **first term** describes the hydrostatic delay, and can be calculated as:

$\Delta\Psi_{hydr,\ SAR} = 2 \cdot 10^{-6} \cdot k_1 \cdot \frac{R_d}{g_m} \cdot P_s$ using the ideal gas law $P = \rho \cdot R_d \cdot T$

and the total surface air pressure P_s: $P_s = g_m \cdot \int_0^{+\infty} \rho(s)\, ds$

- For measured surface air pressure P_s, hydrostatic delay can be predicted with an accuracy of 1 mm [7].
- The **second term** can not be modelled as well as hydrostatic delay. A widely used approach for wet path delay was published by [8]:

$$\Delta\Psi_{wet,\ SAR} = 2 \cdot 10^{-6} \cdot \left(\frac{(k'_2 T_m + k_3) e_0 R_d}{T_0 (g_m(\lambda+1) - \beta R_d)}\right) \cdot \left(1 - \frac{\beta h}{T_0}\right)^{\frac{(\lambda+1)g_m}{\beta R_d} - 1}$$

- $k'_2 = 23.3\left[\frac{K}{mbar}\right]$, $k_3 = 3.75 \cdot 10^5\left[\frac{K^2}{mbar}\right]$ are refractive constants, β=6.5[K/km] is the temperature lapse rate, T_0 [K] temperature and e_0 water vapour pressure above sea level, T_m [K] mean temperature of water vapour, h target's height and λ [unitless] average decrease of water vapour.
- Parameters T, P, e, λ, β are modelled [7] considering target height, latitude and day of the year. For every parameters a look up table is calculated accounting for variations of mean T, P, e, λ, β above sea level regarding different latitudes. The slant propagation is estimated by dividing $\Delta\Psi_{\text{tropo, SAR}}$ by cos α_{OffNd}.

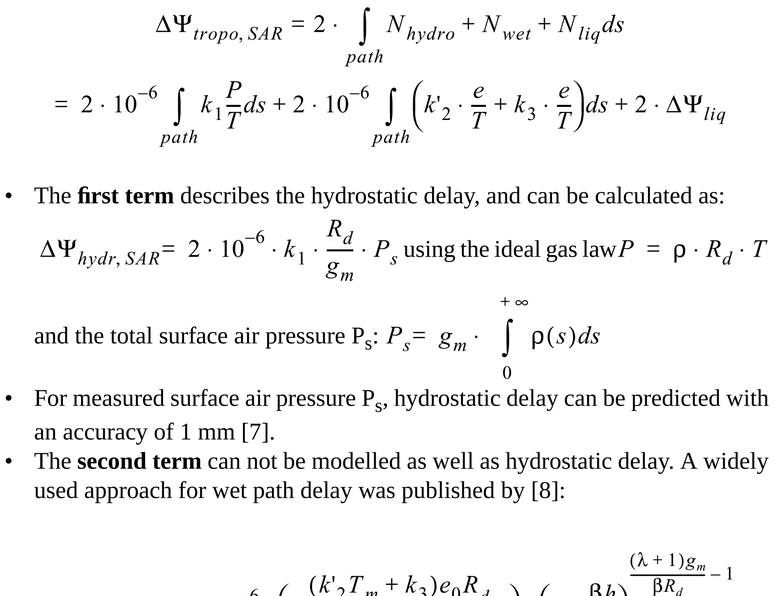

***Figure 3:** Hydrostatic- (left) vs. tropospheric path delay (right).*

Figure 3 shows an example of tropospheric path delay calculated for the ENVISAT-ASAR scene over Lucerne / Zurich. Tropospheric path delay for SAR applications is usually in the range of 4.6 to 5.4 m for hydrostatic delay and 0 to 0.8 m for wet path delay. It can clearly be seen that in the higher regions at the lower right, path delay is about 1 m smaller than in flatter areas in the north. It is evident that, under constant atmospheric conditions, path delay depends mainly on the target's surface height.

Ionosphere:

The ionosphere is located at a height of approximately 50 km -1500 km over the Earth's surface and is characterized by the existence of free electrons and ions that define the refractive index in this area. The degree of ionsation is caused mainly by solar UV radiation and depends on the local atmospheric density. The number of free electrons interacting with the traversing signal cause a path delay that depends on the angle at which the wave enters the layer and on the signal's frequency f. The Total Electron Content (TEC) is usually low at night and highest at about 14:00 local time, when solar radiation is approximately two hours past zenith. This two hour shift depends on the time light needs to ionise the layer to the maximum. The dispersive behaviour of the ionosphere is used by GPS stations to estimate the TEC along the signal path. Global TEC maps are calculated over a network of receiving stations.

Troposphere:

Is the lowest layer of the Atmosphere situated between the Earth's surface and the Stratosphere at a height of 0 km to ~10 km. Tropospheric path delay is caused by variations in the refractive index n as a function of the parameters air pressure P, temperature T and water vapour pressure e.

Propagation of electromagnetic Waves in Medium:

* Fermats' Principle: $\Delta t = \int_{path} dt = \int_{path} \frac{ds}{v} = \min$

* Snell's Law: $n \cdot \sin\alpha_z = const.$

* Effects on signal velocity v: $v = \frac{c_0}{n}$

n: refractive Index, α_z: zenithal incidence angle

IV. Discussion

Using the presented contributions and models for calculating path delay of electromagnetic waves propagating through the atmosphere, we developed a software tool to calculate pixel based path delays for spaceborne L to X-band SAR / radar applications. Even short range atmospheric path delay predictions with an estimated accuracy of at least 50% are possible using an optional ionosphere model in the software.
Figure 2 and 3 show calculated path delay examples from the developed software of an ENVISAT-ASAR scene.
Figure 2 juxtaposes the contribution of the ionospheric path delay and the total path delay. The typical drift in Figure 2a of path delay increasing from the right to the left results from the growing off-nadir angle between satellite and calculated total atmospheric path delays of the scene in Figure 2b are typical for C-band frequencies.
Figure 3a and 3b show the path delays due to the troposphere. While the hydrostatic delay in Figure 3a clearly shows the terrain of the scene, the wet delay has mainly the same behaviour as ionospheric delay (drift to higher amounts with growing off-nadir angle) and is therefore nearly constant. Figure 3b presents the tropospheric delay $\Delta\Psi_{\text{tropo, SAR}} = \Delta\Psi_{\text{hydro, SAR}} + \Delta\Psi_{\text{wet, SAR}}$. The difference between Figure 3a and 3b is mainly a shift in scale, visible as a small difference in brightness.
The software is intended to calculate atmospheric path delays for TerraSAR-X. Total path delays for X-band frequencies would be approximately 0.4 m smaller for the outlined example due to the smaller influence of the ionosphere at that shorter wavelength. The presented ENVISAT-ASAR example demonstrates the tool's adaptive and comparative capabilities.

V. Conclusions

High resolution SAR sensors such as the upcoming TerraSAR-X depend on accurate data calibration to provide the most accurate geolocation possible. Atmospheric path delays therefore have to be considered [1]. We developed a software tool with the presented models and path delay contributions that calculates for spaceborne SAR / radar applications the expected path delay for every single pixel within a scene. This software tool is designed to be easily integrated into other software environments, enabling improved a-priori knowledge of the geometry of a SAR acquisition.

Acknowledgment

This work was founded by the German Aerospace Centre (DLR) through Contract No. 523/65655831.

References

[1] Frey, O.; Small, D.; Meier, E.; Nüesch, D. and Roth, A.: *Geometric Error Budget Analysis for TerraSAR-X*. Proc. EUSAR, 2004.
[2] Hanssen, R. F.: *Radar Interferometry.* Vol.2,Dordrecht, Boston, London: Kluwer Academic Publishers, 2001.
[3] Schaer, S.: *Mapping and Predicting the Earth's Ionosphere using the Global Positioning System*. Geodätisch- geophysikalische Arbeiten in der Schweiz, 1999.
[4] Klobuchar, J.A.: *Ionospheric Time Delay Algorithm for Single Frequency GPS Users.* IEEE Transactions on Aerospace and Electronic Systems, Vol.23, pp. 325-331, 1987.
[5] Saastamoinen, J.: *Contributions to the Theory of Atmospheric Refraction*. Bulletin Geodesique, No. 105. No. 106, No. 107, 1973.
[6] Hopfield, H.: *Tropospheric Range Error at Zenith.* Committee on Space Research, 14th Plenary Meeting, working group 1, id.number a.15, edited by Applied Physics Laboratory, The Johns Hopkins University, Maryland, 1971.
[7] Collins, P. and Langley, R.: *Limiting Factors in Propagation Delay Error Modelling for GPS Airborne Navigation*. The Institute of Navigation 52nd Annual Meeting, Cambridge, USA, 1996.
[8] Askne, J. and Nordius, H.: *Estimation of Tropospheric Delay for Microwaves from Surface Weather Data*. Radio Science, Vol.22, No. 3, pp. 379-386, 1987.